Characterizing Multiscale Mechanical Properties of Brain Tissue Using Atomic Force Microscopy, Impact Indentation, and Rheometry

Citation: Canovic, Elizabeth Peruski; Qing, Bo; Mijailovic, Aleksandar S.; Jagielska, Anna; Whitfield, Matthew J.; Kelly, Elyza; Turner, Daria; Sahin, Mustafa and Van Vliet, Krystyn J. "Characterizing Multiscale Mechanical Properties of Brain Tissue Using Atomic Force Microscopy, Impact Indentation, and Rheometry." Journal of Visualized Experiments no. 115 (September 2016): e54201 © 2016 Journal of Visualized Experiments

As Published: http://dx.doi.org/10.3791/54201

Publisher: MyJoVE Corporation

Persistent URL: http://hdl.handle.net/1721.1/109802

Version: Final published version: final published article, as it appeared in a journal, conference proceedings, or other formally published context

Video Article

Characterizing Multiscale Mechanical Properties of Brain Tissue Using Atomic Force Microscopy, Impact Indentation, and Rheometry

Elizabeth Peruski Canovic[1], Bo Qing[2], Aleksandar S. Mijailovic[3], Anna Jagielska[2], Matthew J. Whitfield[2], Elyza Kelly[4], Daria Turner[4], Mustafa Sahin[4], Krystyn J. Van Vliet[1,2]

[1]Department of Materials Science and Engineering, Massachusetts Institute of Technology

[2]Department of Biological Engineering, Massachusetts Institute of Technology

[3]Department of Mechanical Engineering, Massachusetts Institute of Technology

[4]Department of Neurology, The F.M. Kirby Neurobiology Center, Boston Children's Hospital, Harvard Medical School

Correspondence to: Krystyn J. Van Vliet at krystyn@mit.edu

URL: http://www.jove.com/video/54201
DOI: doi:10.3791/54201

Keywords: Neuroscience, Issue 115, brain tissue, mechanics, elastic modulus, viscoelasticity, indentation, impact indentation, rheology, neuroscience, autism, multiple sclerosis, mouse

Date Published: 9/6/2016

Citation: Canovic, E.P., Qing, B., Mijailovic, A.S., Jagielska, A., Whitfield, M.J., Kelly, E., Turner, D., Sahin, M., Van Vliet, K.J. Characterizing Multiscale Mechanical Properties of Brain Tissue Using Atomic Force Microscopy, Impact Indentation, and Rheometry. *J. Vis. Exp.* (115), e54201, doi:10.3791/54201 (2016).

Abstract

To design and engineer materials inspired by the properties of the brain, whether for mechanical simulants or for tissue regeneration studies, the brain tissue itself must be well characterized at various length and time scales. Like many biological tissues, brain tissue exhibits a complex, hierarchical structure. However, in contrast to most other tissues, brain is of very low mechanical stiffness, with Young's elastic moduli E on the order of 100s of Pa. This low stiffness can present challenges to experimental characterization of key mechanical properties. Here, we demonstrate several mechanical characterization techniques that have been adapted to measure the elastic and viscoelastic properties of hydrated, compliant biological materials such as brain tissue, at different length scales and loading rates. At the microscale, we conduct creep-compliance and force relaxation experiments using atomic force microscope-enabled indentation. At the mesoscale, we perform impact indentation experiments using a pendulum-based instrumented indenter. At the macroscale, we conduct parallel plate rheometry to quantify the frequency dependent shear elastic moduli. We also discuss the challenges and limitations associated with each method. Together these techniques enable an in-depth mechanical characterization of brain tissue that can be used to better understand the structure of brain and to engineer bio-inspired materials.

Video Link

The video component of this article can be found at http://www.jove.com/video/54201/

Introduction

Most soft-tissues comprising biological organs are mechanically and structurally complex, of low stiffness compared to mineralized bone or engineered materials, and exhibit non-linear and time-dependent deformation. Compared to other tissues in the body, brain tissue is remarkably compliant, with elastic moduli E on the order of 100s of Pa [1]. Brain tissue exhibits structural heterogeneity with distinct and interdigitated gray and white matter regions that also differ functionally. Understanding brain tissue mechanics will aid in the design of materials and computational models to mimic the response of the brain during injury, facilitate prediction of mechanical damage, and enable engineering of protective strategies. Additionally, such information can be used to consider design targets for tissue regeneration, and to better understand structural changes in brain tissue that are associated with diseases such as multiple sclerosis and autism. Here, we describe and demonstrate several experimental approaches that are available to characterize the viscoelastic properties of mechanically compliant tissues including brain tissue, at the micro-, meso-, and macro-scales.

At the microscale, we conducted creep-compliance and force relaxation experiments using atomic force microscope (AFM)-enabled indentation. Typically, AFM-enabled indentation is used to estimate the elastic modulus (or instantaneous stiffness) of a sample [2-4]. However, the same instrument can also be used to measure microscale viscoelastic (time- or rate-dependent) properties [5-10]. The principle of these experiments, shown in **Figure 1**, is to indent an AFM cantilevered probe into the brain tissue, maintain a specified magnitude of force or indentation depth, and measure the corresponding changes in indentation depth and force, respectively, over time. Using these data, we can calculate the creep compliance J_C and relaxation modulus G_R, respectively.

At the mesoscale, we conducted impact indentation experiments in fluid-immersed conditions that maintain the tissue structure and hydration levels, using a pendulum-based instrumented nanoindenter. The experimental setup is illustrated in **Figure 2**. As the pendulum swings into contact with the tissue, probe displacement is recorded as a function of time until the oscillating pendulum comes to rest within the tissue.

From the resulting damped harmonic oscillatory motion of the probe, we can calculate the maximum penetration depth x_{max}, energy dissipation capacity K, and dissipation quality factor Q (which relates to the rate of energy dissipation) of the tissue [11,12].

At the macroscale, we used a parallel plate rheometer to quantify the frequency dependent shear elastic moduli, termed the storage modulus G' and loss modulus G'', of the tissue. In this type of rheometry, we apply a harmonic angular strain (and corresponding shear strain) at known amplitudes and frequencies and measure the reactional torque (and corresponding shear stress), as shown in **Figure 3**. From the resulting amplitude and phase lag of the measured torque and geometric variables of the system, we can calculate G' and G'' at applied frequencies of interest [13,14].

Protocol

Ethics Statement: All experimental protocols were approved by the Animal Research Committee of Boston Children's Hospital and comply with the National Institutes of Health Guide for the Care and Use of Laboratory Animals.

1. Mouse Brain Tissue Acquisition Procedures (for AFM-enabled indentation and impact indentation)

1. Prepare a ketamine/xylazine mixture to anesthetize the mice. Combine 5 ml ketamine (500 mg/ml), 1 ml xylazine (20 mg/ml) and 7 ml of 0.9% saline solution.
2. Inject mouse (Breed: TSC1; Syn-Cre; plp-eGFP; Age: p21; Sex: Male or Female) with 7 µl per gram bodyweight of the ketamine/xylazine solution.
3. Once the mouse is fully anesthetized, as demonstrated by a lack of response to toe and tail pinches, euthanize the mouse by decapitation using large dissection scissors.
4. Remove the skull by cutting down the middle using smaller dissection scissors. Starting at the cerebellum, remove pieces of the skull using curved forceps. After removing the skull, extract the brain by using a flat spatula to lift the brain, starting at the cerebellum, and place the brain on a Petri dish. Remove the cerebellum from the brain using a razor blade.
5. If using a whole brain for impact indentation tests on fresh tissue, transfer brain into a round-bottomed tube with CO_2-independent nutrient medium for adult neural tissue on ice and proceed to section 4. Otherwise proceed to step 1.6 for slicing procedures.
6. Adjust the vibratome settings to a speed of 0.7 mm/sec, a vibration frequency of 70 Hz, and a slice thickness of 350 µm. Surround the vibratome dish with ice. Place a dab of superglue onto the vibratome plate and mount brain so that coronal slices can be cut, with the brain oriented to cut through the dorsal side first.
7. Fill the vibratome dish with enough Dulbecco's phosphate-buffered saline (DPBS) to just submerge the brain. Raise the dish on the vibratome so that blade is just submerged in the DPBS.
8. Press start to begin slicing coronal brain sections 350 µm thick.
9. Using paintbrushes to avoid damage to the tissue, transfer the brain slices from the vibratome DPBS bath and into a round-bottomed tube with CO_2-independent nutrient medium for adult neural tissue on ice and perform measurements on fresh tissue within 48 hr. To begin AFM-enabled indentation experiments, proceed to section 3.

2. Pig Brain Tissue Acquisition Procedures (for rheology)

1. Obtain a sagittally sliced porcine half brain within ~1 hr of sacrifice from a local butcher. Place the half brain in CO_2-independent nutrient medium for adult neural tissue, and store on ice.
2. Use a razor blade or scalpel to make a ~5 mm thick coronal brain slice and store in CO_2-independent nutrient medium for adult neural tissue. Ensure that the slice surface is as flat as possible. Use careful lateral motions with razor/scalpel during sectioning.
3. Store pig brain tissue in CO_2-independent nutrient medium for adult neural tissue on ice and perform rheometry measurements (section 5) on fresh tissue within 48 hr.

3. Atomic Force Microscope-enabled Indentation

1. Prepare 60 mm-diameter Petri (P60) dishes with a mussel-derived bioadhesive according to the manufacturer's instructions.
    1. Prepare a stock of neutral buffer solution consisting of 0.1 M sodium bicarbonate in sterile water with an optimal pH of 8.0. Filter-sterilize (0.2 micron) the sodium bicarbonate buffer and store at 4 °C.
    2. In a laminar flow hood, mix a solution of 6.25% mussel-derived bio-adhesive and 3.125% NaOH in the sodium bicarbonate buffer.
    3. Pipette 100µl of the bio-adhesive solution from 3.1.2 onto a 60 mm-diameter Petri (P60) dish and use pipette tip to spread solution into a 3-5 cm diameter circle.
    4. Leave P60 dishes uncovered in laminar flow hood and let solution dry (~30 min). Wash dishes 1x with PBS and 2x with sterile water. Let dishes air dry in laminar flow hood and store in a sealed plastic bag at 4 °C for up to 1 month.

2. Calibrate the AFM and set-up brain sample in the AFM.
   NOTE: Follow AFM calibration instructions as per the manufacturer.
    1. Carefully load an AFM probe with a nominal spring constant of 0.03 N/m and a 20 µm-diameter borosilicate bead into the probe holder.
    2. Calibrate the spring constant and inverse optical lever sensitivity (InvOLS) of the AFM cantilever using the thermal tune method [15,16].
       NOTE: Once the spring constant for an AFM probe is calculated, it should remain constant with repeated use. However, the cantilever InvOLS will need to be recalibrated each time the laser is realigned with the cantilever. Additionally, calibration should be performed against a substrate several order of magnitude stiffer than the cantilever, such as polystyrene.
    3. Turn on the stage-mounted heater and set temperature to 37 °C.
    4. Mount the brain slice onto the P60 dishes prepared in section 3.1.

1. Gently pour a 350 µm thick brain slice, as well as the CO_2-independent medium from the round bottom flask into a P60 dish coated with the mussel-derived bioadhesive.
2. By gently tilting the P60 dish, position the brain slice in the center of the dish. If necessary, slowly pipette medium from a manual pipetter to unfold a brain slice that has folded over on itself or better position the brain slice in the center of the dish.
3. Carefully remove excess media using a P1000 pipetter (do not use the vacuum).
4. Place cover on P60 dish and let the brain slice adhere for 20 min.

5. Remove the AFM head, place the brain slice mounted in the P60 dish on the AFM stage, and add ~2 ml pre-warmed CO_2-independent medium.
6. Carefully add a drop of media onto the AFM probe to protect it from breaking due to surface tension when it is lowered into the media surrounding the brain slice.
7. Reposition the AFM head onto the stage, and begin lowering the head until it is submerged into the media.
8. Using the top-view CCD camera, reposition the laser onto the cantilever.
   NOTE: The alignment of the laser on the cantilever will have changed slightly due to the difference in refractive index of air and medium.
9. Wait 5 min for the cantilever to adjust to being submerged in a warm liquid, then reset the mirror alignment to a free deflection of 0 V.
10. Run a thermal spectrum on the AFM probe according to the manufacturer's instructions[16]. Use the fit of the first thermal peak to re-calculate the AFM probe's InvOLS in media.
11. Using the optical microscope, move the sample stage such that the brain region of interest below the AFM probe.
    NOTE: The corpus callosum will appear dark as it is more opaque than the surrounding gray matter. The cortex is superior to the corpus callosum.
12. Reset the mirror alignment to a free deflection of 0 V.
13. On the Sum and Deflection Meter in the AFM software, click "Engage" to engage the AFM head.
14. Using the position dial on the AFM head, lower the head until contact between the cantilever and sample is made.

3. (Optional) If desired, measure the elastic modulus of the sample, as described previously [4,17,18].
4. Conduct creep compliance experiments.
   1. Construct an applied force function in the software's function editor. The force function consists of a 0.1 sec ramp to a set point of 5 nN and hold it for 20 sec, followed by a 1 sec ramp down to an applied force of 0 nN.
      1. On the Indentation Master Panel, under the indentation method, select "Load" for Indenter Mode; "N" for units; and "Function editor" for Indenter Function.
      2. In the function editor, on the Segment Parms Panel, create an applied force function segment that starts at 0 nN, ends at 5 nN, with a time of 0.1 sec. Click "Insert -->".
      3. For the next segment, set start to 5 nN, end to 5 nN, and time to 20 sec. Click "Insert -->."
      4. For the final segment, set start to 5 nN, end to 0 nN, and time to 1 sec. Click "Draw" and close the Function Editor window.

   2. On the Force Tab of the Master Panel, check "indenter ramp after trigger" and set the applied force function to trigger after reaching a trigger point of 0.1 V.
   3. Click "Single Force" on the bottom of the Force Tab of the Master Panel, which will trigger the constructed-applied force function for creep compliance.
   4. After the single force indentation is finished, raise the AFM head so that it is out of contact with the sample and then re-engage the head and re-zero free deflection.
   5. Reposition the sample stage to locate a new area of interest, and lower the AFM head to make contact. NOTE: The AFM head must be retracted from sample surface when the sample stage is moved. Failure to do so can result in damage to the delicate AFM cantilever.
   6. Repeat steps 3.4.3-3.4.5 until desired amount of data has been collected.

5. Conduct force relaxation experiments.
   1. Construct an applied indentation function in the software's function editor. The indentation function consists of a 0.1 sec ramp to a set point of 3 µm and hold it for 20 sec, followed by a 1 sec ramp down to an indentation depth of 0 µm.
      1. On the Indentation Master Panel, under the indentation method, select "Indentation" for Indenter Mode; "m" for units; and "Function editor" for Indenter Function.
      2. In the function editor, on the Segment Parms Panel, create an applied force function segment that starts at 0 µm, ends at 3 µm, with a time of 0.1 sec. Click "Insert -->".
      3. For the next segment, set start to 3 µm, end to 3 µm, and time to 20 sec. Click "Insert -->."
      4. For the final segment, set start to 3 µm, end to 0 µm, and time to 1 sec. Click "Draw" and close the Function Editor window.

   2. On the Force Tab of the Master Panel, check "indenter ramp after trigger" and set the applied force function to trigger after reaching a trigger point of 0.1 V.
   3. Click "Single Force" on the bottom of the Force Tab of the Master Panel, which will trigger the constructed-applied indentation function for force relaxation.
   4. After the single force indentation is finished, raise the AFM head so that it is out of contact with the sample and then re-engage the head and re-zero deflection.
   5. Reposition the stage to locate a new area of interest, and lower the head to make contact.
   6. Repeat steps 5.3-5.5 until desired amount of data has been collected.

6. Conclude experiments and clean-up.
   1. After concluding experiments, raise the AFM head and remove it from the sample.
   2. Use a lab tissue to carefully remove excess liquid without touching the cantilever.
   3. Carefully clean the AFM cantilever holder using a small amount of ethanol. Do not expose the delicate electronics on the cantilever holder to ethanol. Remove the AFM cantilever and place in a storage container.

4. Dispose of the brain tissue sample by following appropriate biosafety protocols.

7. Using MATLAB, calculate creep compliance and force relaxation moduli using indenter geometry, according to the solution derived by Lee and Radok, 1960 [19].
   1. Calculate force *F* and indentation depth δ from data on the cantilever position *z*, deflection *d*, and spring constant, k_c $\delta = d - z$ and $F = k_c d$.
   2. Locate the contact point along the indentation curve using the algorithm described in Lin *et al.* [20].
   3. Define a window of interest for data analysis. The window of interest is the region where either force (for creep compliance) or indentation depth (for force relaxation) is maintained at a setpoint value (*i.e.*, Region 3 as shown in **Figure 1C,D**).
   4. For creep compliance experiments, calculate the experimental creep compliance modulus, $J_c(t)$, in response to a step load $F(t) = F_0 H(t)$:

      $J_C(t) = \frac{16\sqrt{R}}{3F_0}\delta^{3/2}(t)$,

      where *H(t)* is the Heavyside step function and *R* is the radius of the spherical probe.
   5. For force relaxation experiments, calculate the experimental force relaxation modulus, $G_R(t)$, in response to a step indentation depth $\delta(t) = \delta_0(t)$:

      $G_R(t) = \frac{3}{16\sqrt{R}\delta_0^{3/2}}F(t)$.

4. Impact Indentation

1. Calibrate the instrumented nanoindenter and adjust default settings to enable dynamic impact experiments on hydrated brain tissues according to the manufacturer's instructions.
   1. Mount a spherical probe by sliding it onto the pendulum using tweezers.
   2. Glue a fused quartz sample onto the sample post, which is screwed into the translational stage.
   3. Go to the Calibration menu and select "Liquid Cell." Follow the software's instructions to make contact with the fused quartz sample.
   4. Select "Normal" for the Indenter Type and use the default value of 0.05 mN for the Indenter Load. Click "Continue" to perform the calibration for the normal indenter configuration.
   5. Move the sample stage back by at least 5 mm. Mount the lever arm, which allows the probe to be lowered into the liquid cell, and repeat the liquid cell calibration in the new configuration by selecting "Liquid Cell" for the Indenter Type. Click "Continue" to obtain the Liquid Cell Calibration Factor.
   6. Activate the Liquid Cell software option by going to the Experiment menu and selecting "Special Options." Use the latest calibration value.
   7. Increase the capacitor plate spacing as this will lead to a greater maximum measurable depth, which is necessary when testing highly compliant materials.
      1. Under the System menu, select "Non Protected Settings" and "Machine Parameters" to change the pendulum test load rate, zero load rate, and standby ramp offset to 0.5 mN/sec, 0.1 mN/sec, and 3 V, respectively.
      2. With a wrench, turn the three nuts that control the capacitor plate spacing clockwise in small increments.
      3. After each complete clockwise turn, select "Bridge Box Adjustment" under the Maintenance menu and obtain a good pendulum test, which will require moving the counter-balance weight away from the pendulum.
      4. Repeat steps 4.1.7.2-4.1.7.3 until the approximate depth calibration reads a value of 70,000 nm/V or higher.
   8. Position a new limit stop at the bottom of the pendulum that can be switched on and off via a power supply. Retract the original limit stop sitting behind the pendulum to remove a potential obstruction of the pendulum motion and allow for higher impact velocities as well as higher penetration depths into compliant samples.
   9. Allow the cabinet to reach thermal equilibrium (takes approximately 1 hr).
   10. While the cabinet equilibrates, go back to the System menu and select "Non Protected Settings" and "Machine Parameters." Set the depth calibration (dcal) contact velocity to 1 µm/sec, the primary indentation contact velocity to 3 µm/sec, and the ultra low load contact velocity to 1 µm/sec.
   11. Under the Calibration menu, perform a standard depth calibration in this new configuration.
   12. Turn on the power supply for the solenoid and set it to 10 V. Go to the Experiment menu and select "Impact" and "Adjust Impulse Displacement." Follow the software instructions (automatic prompts) to calibrate the swing distance of the pendulum.

2. Mount the mouse brain tissue in the liquid cell.
   1. After harvesting the whole brain from step 1.5, store it immediately in CO_2-independent nutrient medium for adult neural tissue media on ice.
   2. When the impact indentation setup is fully complete, carefully transfer the brain into a petri dish along with CO_2-independent medium. Slice the brain into 6 mm thick sections with flat surfaces on either side.
   3. Adhere the sliced tissue to the aluminum sample post with a thin layer of cyanoacrylate adhesive.
   4. Slide the liquid cell over the second O-ring on the sample post, and fill the liquid cell with 5 ml of CO_2-independent medium to fully immerse the tissue. This sample post is then carefully mounted onto the translational stage inside the instrumented nanoindenter.

3. Measure the impact response of the brain tissue.
   1. If necessary, remove the spherical probe and replace it with the probe of interest without removing the lever arm.
   2. Under the System menu, select "Non Protected Settings" and "Machine Parameters." Change the primary impact contact velocity to 5 µm/sec.
   3. With the sample bath low (-z direction) and far away from the pendulum (+x direction), move in the -x direction until the tip on the lever arm is properly located above the bath. Move in the +z direction until the tip is fully submerged in the bath and in front of the sample.

4. Using the sample stage control window, make contact carefully and then back the stage away from the sample surface by approximately 30 µm.
5. Under the Experiment menu, click "Impact" to set up an impact experiment. Choose a specific impulse load that will relate directly to the resulting impact velocity based on the swing distance calibration. Run the scheduled experiment.
6. When the pendulum swings back and the sample surface continues to move to the measurement plane, turn the bottom limit stop switch off.
7. Observe as the pendulum swings forward to impact the sample. The displacement of the probe as a function of time will be recorded by the software.
8. When the xyz stage window appears, turn the limit stop switch back on.
9. Repeat steps 3.4-3.8 to test as many different loads and locations as needed.

4. Analyze the acquired displacement vs. time response of the pendulum using customized MATLAB scripts to determine the maximum penetration depth x_{max}, energy dissipation capacity K, and dissipation quality factor Q.[11]
   1. Go to the Analysis menu and export the data in a text file.
   2. Take the time derivative of the displacement profile to obtain velocity as a function of time. Set zero displacement as the contact point x_{o1}.
      NOTE: Impact velocity v_{in} is the maximum velocity immediately prior to contact. x_{max} corresponds to the deformation at which the probe velocity first decreases to zero. x_{o2}, which is equivalent to x_r, is the position required to reinitiate contact with the deformed sample in the next cycle. Rebound velocity v_{out} is the velocity at displacement x_r.
   3. Define K (unitless) as the energy dissipated by the sample normalized by the sum of the recovered and dissipated sample energies during the first impact cycle. Calculate K based on the intrinsic properties of the pendulum [21] (such as rotational stiffness and damping coefficient), x_{o1}, x_{max}, x_r, v_{in}, and v_{out}.
      NOTE: For more information, one may consult the work of Kalcioglu *et al.,* 2011.
   4. Since displacement can be described as a damped harmonic oscillatory motion, fit an exponential decay function to the maxima of the displacement vs. time curve.
   5. Calculate Q (unitless) as π multiplied by the number of cycles required for the oscillation amplitude to decrease by a factor of e. A higher Q value means a lower energy dissipation rate.

5. Rheology

1. Set-up and calibrate the rheometer as per the manufacturer's instructions.
   1. Initialize the rheometer by opening the device/control panel. On the control panel tab, click "initialize."
   2. Mount the 25 mm-diameter measurement plate (PP25) and the thermal system.
   3. (Optional) To reduce slip between rheometer plates and the tissue, cut out adhesive sandpaper slices that match the shape of the top rheometer plate and adhere the sandpaper to the top and bottom plate.
   4. Make contact between the top and bottom plate by clicking "set zero gap" on the control panel.
   5. Zero the normal force transducer by clicking "reset normal force."
   6. Conduct an inertia test by opening the service tab on the control panel, clicking "measurement system," and then clicking "inertia test". Record the old and new inertia. Verify that the inertia is within the allowable limit for the probe, as listed by the manufacturer.

2. Load sample into rheometer.
   1. After harvesting the tissue and slicing a coronal segment of the pig brain to ~5 mm thickness, store it on ice in CO_2-independent medium.
   2. Place the brain between the two plates. Remove large water droplets from the top and bottom surface of the sample to prevent slippage, but do not dry out the sample.
   3. Slowly lower the measurement plate until the plate is in full contact with the top surface of the tissue and the measured normal force is consistent at 0.01 mN after a 5-10 min relaxation period.
      1. In the control panel, enter successively lower heights in the measurement position box and click "measurement position" to slowly lower the measurement plate.
      2. When within a millimeter of contact with the tissue, lower the measurement plate in 0.1 mm increments until the plate is fully in contact with the top surface of the tissue. Ensure that the measured-normal force is consistently at 0.01 mN after a 5-10 min relaxation period.
      3. Record the initial measured normal force. Repeated measurements should be taken at the same compressive stresses/strains.
   4. Trim the sample with a plastic blade if the sample exceeds the diameter of the plate. Pipette a small volume (~1-2 ml) of media on the edges of the sample to hydrate the tissue.
   5. (Optional) Lower the thermal hood. On the control panel, set the temperature to 37 °C and click "set".

3. Perform an amplitude sweep to establish the linear viscoelastic range of the material (*i.e.,* the shear strains at which G' and G'' are constant) at frequencies of interest (*e.g.,* 1 rad/sec).
   1. Select "file/new". Under the gel tab select "Amplitude sweep: LVE-range." Select window and click "Measurement 1: Amplitude sweep." Double click on the oscillation box. Enter the initial and final strain (*e.g.,* 0.01 to 105), the frequency (*e.g.,* 1 rad/sec) and the number of points per decade (*e.g.,* 6 points/dec). Select "ok" and click start."
   2. Repeat this procedure for several slices with repeated trials to ensure consistency of the linear elastic range. The axial compression of the sample should remain constant between samples.

4. Conduct a frequency sweep of the tissue at a strain in the linear viscoelastic range of the tissue (*e.g.,* 1% strain) [22], and at a frequency range of interest (*e.g.*, 0.1-100 rad/sec).

1. Click "file/new" and under the gel tab select "Frequency sweep." Click window/Measurement 1: Frequency sweep. Double click on the oscillation box. Enter the frequency range (*e.g.*, 0.1 to 100 rad/sec), the strain (*e.g.*, 1% strain) and the number of points per decade (*e.g.*, 6 points/dec). Select "ok" and click "start" to initiate the frequency sweep.

5. Repeat frequency sweep (step 5.4) in duplicates or triplicates.
6. Review the data that are automatically calculated and exported by the rheometer: *G′* and *G″* as a function of frequency (frequency sweep) or shear strain (amplitude sweep). NOTE: *G′* and *G″* are calculated from the sample's (maximum) reactional torque amplitude T'_0, and rotational displacement angle (or deflection angle) φ_0, and phase lag Φ, of the sample's response to the applied oscillatory strain (**Figure 3**):

$$G' = \frac{2T_0 h}{\pi \varphi_0 R^4} \cos \Phi$$

$$G'' = \frac{2T_0 h}{\pi \varphi_0 R^4} \sin \Phi$$

where *R* and *h* are the radius and height of the sample.

Representative Results

Figure 4 shows representative indentation and force vs. time responses (**Figure 4B,E**) for creep compliance and force relaxation experiments, given an applied force or indentation depth (**Figure 4A,D**), respectively. Using these data and the geometry of the system, the creep compliance $J_c(t)$ and force relaxation moduli $G_R(t)$ can be calculated for different regions of the brain (**Figure 4C,F**). While previous studies have shown a difference between the elastic moduli of different areas of the brain[23], the viscoelastic properties measured in this way for mouse brain tissue slices do not show interregional variation within a given tissue slice.

Impact indentation measures the mechanical properties of the tissue at high rates of spatially and temporally concentrated loading. The results of these experiments provide information about how the tissue dissipates energy in response to traumatic injury or intentional deformation associated with surgery. The damped oscillatory motion of the impact indentation probe (**Figure 2B**) provides information to calculate the maximum penetration depth x_{max} (**Figure 5A**), energy dissipation capacity *K* (**Figure 5B**) and energy dissipation rate *Q* (**Figure 5C**) of the tissue. Penetration depth measures the deformation resistance, which strongly correlates with the tissue's elastic modulus: stiffer tissues exhibit smaller penetration depths for a given impact velocity and impact energy. Energy dissipation capacity is a unitless measure of the extent to which the tissue dissipates the impact energy during the first impact cycle. Dissipation quality factor measures how many cycles occur before the oscillations from impact are damped significantly — this relates directly to the rate of energy dissipation, though this is not expressed in units of time. These three impact response parameters can be quantified at different impact velocities, which provides a means to study the rate-dependent properties of the tissue.

Figure 6 shows macroscale *G′* and *G″* for frequencies ranging from 0.1 rad/sec to 50 rad/sec. The storage modulus is nearly an order of magnitude larger than the loss modulus at low frequencies. However, the ratio between storage and loss moduli decreases as frequency increases. This indicates that elastic properties dominate the behavior of brain tissue, since the storage modulus describes elastic properties and the loss modulus describes viscous losses of the material. At a sufficiently high loading frequency, the storage and loss moduli will equate, indicating the point at which the material begins to flow (*i.e.*, viscous properties dominate the behavior of the sample). For the case of brain tissue measured as illustrated herein, physical limitations of the instrumentation do not allow us to measure material properties at higher frequencies.

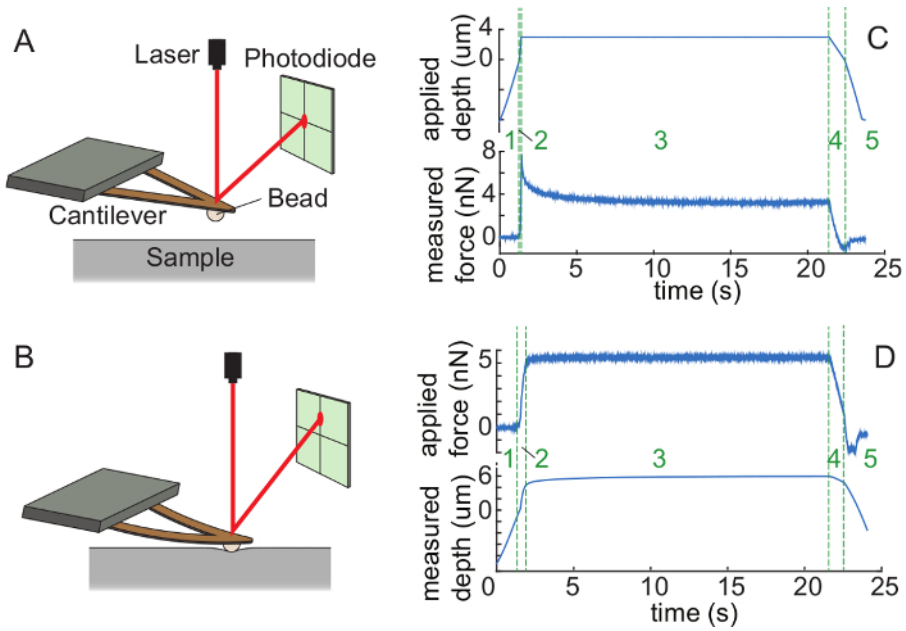

Figure 1. Illustration of AFM-enabled creep compliance and force relaxation experiments. (**A**) AFM-enabled indentation is conducted using a flexible cantilever with a spherical bead of nano- to microscale radius attached to the free-end. (**B**) During indentation, cantilever deflection is measured using a laser reflected off the end of the cantilever and onto a photodiode. (**C**) Force relaxation experiments are conducted by indenting the cantilever to a constant applied depth, while the force decay with respect to time is measured. (**D**) Creep compliance measures the changing indentation depth of the cantilever with a constant applied force. (C) and (D) have been divided into five regions (green text): (1) Approach of the AFM probe to the sample surface, (2) Contact with sample and ramp up to a setpoint indentation/force, (3) maintenance of the setpoint indentation/force, (4) ramp down and (5) retraction of the AFM probe from the sample surface. Please click here to view a larger version of this figure.

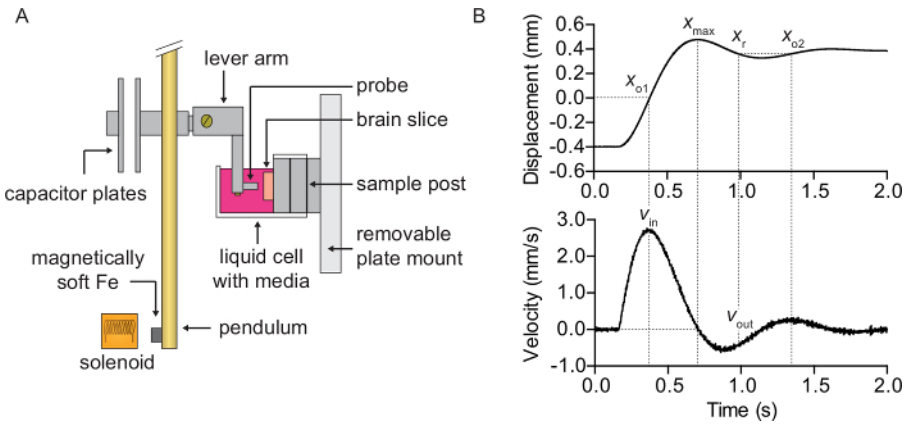

Figure 2. Illustration of impact indentation experiments. (**A**) Schematic of impact indentation, illustrating the ability to conduct experiments in fully hydrated conditions. (**B**) Representative probe displacement profile as a function of time collected from a mouse brain slice and the corresponding velocity profile. Key measured displacement and calculated velocity parameters used to quantify energy dissipation are indicated. Please click here to view a larger version of this figure.

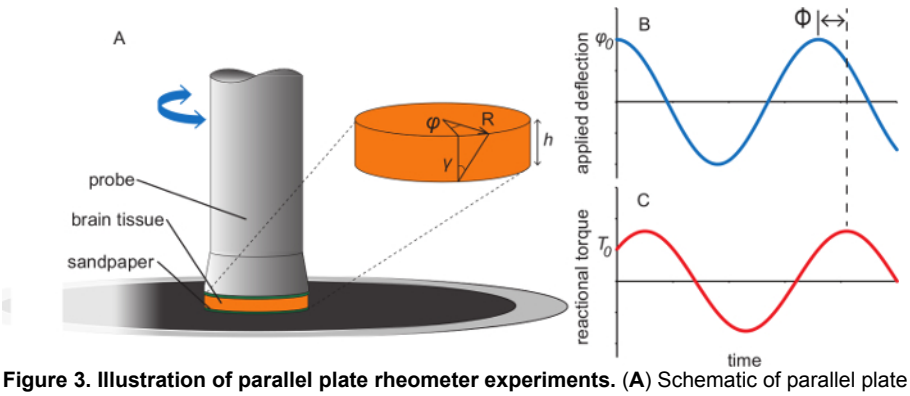

Figure 3. Illustration of parallel plate rheometer experiments. (**A**) Schematic of parallel plate rheometer experiment and definitions related to applied oscillatory shear strain. (**B**) Representative applied strain and resulting stress as a function of time. Shear storage modulus *G*' and shear loss modulus *G*" are calculated via the strain amplitude $\square_0$, torque amplitude *T'*$_0$, phase lag Φ, probe and sample radius *R*, and sample height *h*. Please click here to view a larger version of this figure.

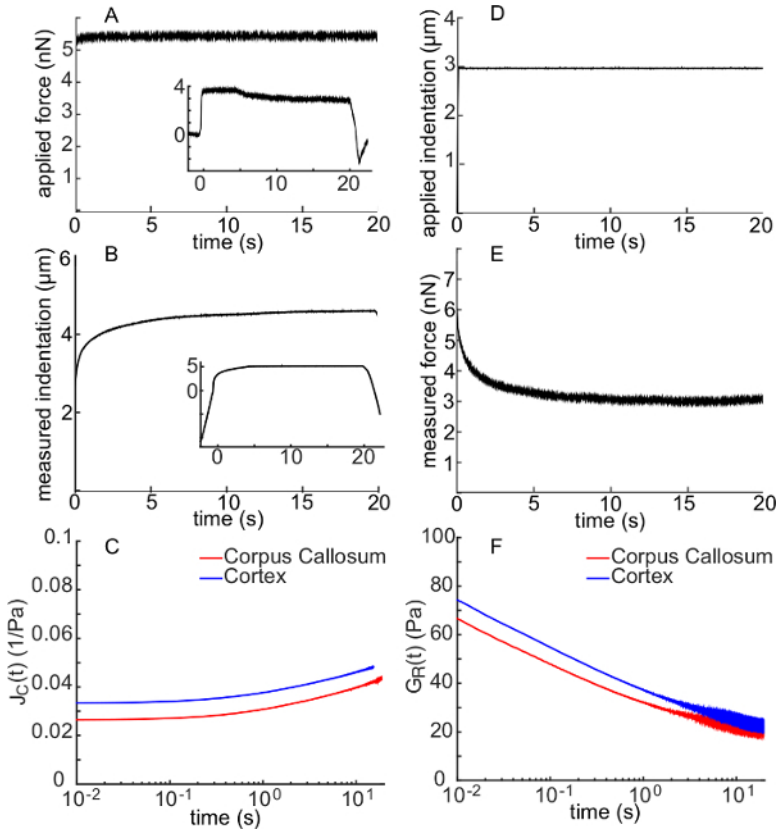

Figure 4. Representative data from creep compliance and force relaxation experiments. (**A**, **B**) From the raw data in **Figure 1**, a region of interest is defined for creep compliance as the time where applied force remains constant **(A)** while the indentation depth is measured **(B)**. The inset in **(A)** shows data from an unsuccessful experiment where the AFM piezo was unable to maintain the applied force and the inset in (B) shows the corresponding indentation response, which is qualitatively similar to the data of a successful experiment shown in **(B)**. (**C**) With data from the applied force, measured indentation, and knowledge of the geometry of the probe, creep compliance $J_c(t)$ is computed. (**D**,**E**) In force relaxation, indentation depth is held constant **(D)**, while force vs. time is measured **(E)**. (**F**) Using these data, force relaxation modulus $G_R(t)$ can be computed. Creep compliance and force relaxation experiments can be conducted on anatomically distinct regions of the brain, such as the corpus callosum (red) and cortex (blue). Data in **(C, F)** are an average of measurements from n=5 mice. Please click here to view a larger version of this figure.

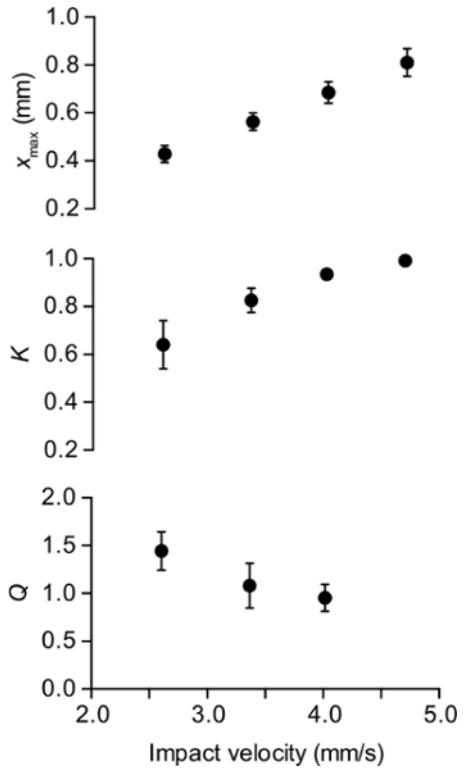

Figure 5. Representative data from impact indentation experiments. Maximum penetration depth x_{max}, energy dissipation capacity *K*, and dissipation quality factor *Q* of mouse brain tissue are calculated from raw displacement profiles obtained at different impact velocities. Data are represented as mean ± standard deviation (n = 18 replicate measurements per point). Please click here to view a larger version of this figure.

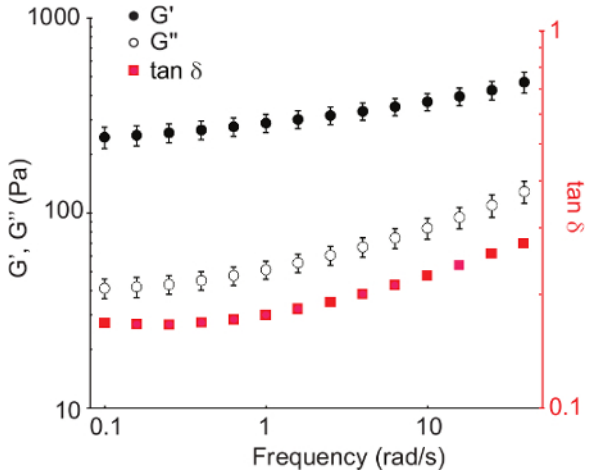

Figure 6. Representative data from rheometry experiments. Storage *G'* and loss *G''* moduli of from coronal slices of pig brains. The quantity tanδ is calculated as the ratio of loss to storage modulus. Data are represented as mean ± standard deviation (n = 4 replicate measurements per point). Please click here to view a larger version of this figure.

Discussion

Each technique presented in this paper measures different facets of brain tissue's mechanical properties. Creep compliance and stress relaxation moduli are a measure of time-dependent mechanical properties. The storage and loss moduli represent rate-dependent mechanical properties. Impact indentation also measures rate-dependent mechanical properties, but in the context of energy dissipation. When characterizing tissue mechanical properties, both AFM-enabled indentation and rheology are commonly used methods. AFM-enabled indentation is particularly useful because in addition to providing time dependent material properties, different experimental parameters can be used to measure cell and tissue elastic modulus [4] and even frequency dependent properties [24], as described previously. However, accurate interpretation of the data and design of experiments can be challenging for compliant, hydrated tissues. While rheometry measures bulk properties of the tissue, AFM-enabled indentation probes microscale volumes relevant to cells' microenvironment. Impact indentation provides a means to quantify specifically how a material deforms in the context of a concentrated, dynamic impact load, which is useful in applications like studying

traumatic brain injury caused by focal impact. While the results from each technique are not directly comparable, the energy dissipation characteristics measured via impact indentation follow the same trends as the shear loss modulus measured via rheology, as discussed below.

In the AFM-enabled indentation of brain tissue illustrated herein, we measured viscoelastic properties using creep compliance and force relaxation. Because of the small scale of the AFM probe, this technique can measure mechanical properties of anatomically distinct areas of the brain, such as the white and gray matter regions of the corpus callosum and cortex, respectively (**Fig. 4**). While there are other techniques for measuring microscale mechanical properties of biological specimens — such as magnetic twisting cytometry, optical tweezers, and microrheology — these techniques have not been successfully used on tissue samples due in part to the relatively strong scattering of light within semi-opaque tissues.

We found that the viscoelastic behavior of brain tissue measured in this manner is qualitatively similar to previously reported results by Elkin & Morrison [26]. While the magnitude of the measured values for relaxation modulus do not agree, this is likely due to the difference in experimental conditions. Elkin & Morrison use a 250 µm diameter flat punch, compared to our 20 µm diameter sphere. Additionally, Elkin & Morrison perform measurements on brain tissue from rats, while we conducted measurements on brain tissue obtained from mice. Despite these differences, both techniques measured heterogeneous mechanical properties within brain tissue, or more specifically, that the white matter of the corpus callosum exhibits a lower relaxation modulus than the gray matter of the cortex in the coronal plane.

It is important to note that while we calculated the creep compliance and force relaxation moduli in response to a requested step load or step indentation, respectively, the experimentally applied load and indentation are not ideal (instantaneous) step functions. Loads and indentations are applied over short timescales (<1 sec), and these loading histories can affect the measured creep and relaxation responses [7,25]. Specifically, assuming an applied step indentation results in slight under-estimation of the relaxation modulus, while assuming an applied step load results in slight over-estimation of the creep compliance modulus. The discrepancies between the actual and calculated elastic moduli will decrease as the ramp rates of the applied loads and indentation increase.

A key step in conducting load relaxation is choosing the proper magnitude of maintained force (*i.e.*, the setpoint corresponding to the photodiode voltage that relates directly to the applied force). The setpoint force for creep compliance must be chosen so that: (1) the response is large enough to produce easily measureable changes in indentation depth; and (2) small enough that the indentation depth required to maintain the setpoint force does not become so large as to drift outside of the range of the AFM piezoelectric actuator that modulates the vertical position of the AFM cantilever base. In the presented protocol, we have suggested a setpoint force of 5 nN, which worked well for our experimental setup. However, if the AFM piezo is unable to maintain that force due to its limited range of motion (see **Fig. 4A**, inset), that value can be lowered. This experimental issue is not encountered with force relaxation experiments that maintain a constant, calculated indentation depth through a feedback loop.

In contrast to the quasi-static AFM-enabled indentation at nanoNewton (nN) scale forces and µm-scale depths, impact indentation applies a concentrated dynamic load of mN-scale forces and measures the specimen's deformation response to depths approaching the millimeter-scale. We have previously used impact indentation to quantify the behavior of the heart and liver [9,11,12] , and observed a similar dependence of energy dissipation response on loading rate for tissues from those organs.

Impact indentation can accommodate probe radii ranging from µm to mm. Additionally, impact indentation experiments can be conducted in fully immersed environments, which allows for the mechanical characterization of hydrated tissues [21]. When testing highly compliant samples such as brain tissue, important considerations must be taken into account. First, the maximum measurable depth into the material is approximately 1 mm, a limitation set by the length scales of the instrument itself; any further pendulum displacement will be physically halted by the collision between the electromagnetic coil located at the top of the pendulum and the stationary magnetic plate. For brain tissue, this limits the highest impact velocity that can be successfully applied to approximately 5 mm/sec. Note that while the impact velocities are on the order mm/s, the corresponding strain energy densities are on the order of kJ/m^3, which approaches ballistic conditions, due to the small dimensions of the probe radius [11]. Second, it can potentially become difficult for the instrument to detect contact between the probe and tissue surface. As the sample stage travels toward the probe, contact is detected when the pendulum is pushed back by the moving sample. However, for highly compliant samples, the pendulum may not be deflected detectably while the probe penetrates into the sample.

To address this problem, we can increase the speed at which the sample stage moves such that there will be a greater momentum during contact to drive the pendulum back. The sample should also be as flat as possible, to further minimize any errors in detecting the proper contact point. Lastly, note that the impact load is not a true impulse load, in that the electromagnetic current at the pendulum top continues to supply a driving force for penetration after the first impact event. As a result, creep may occur especially at the higher loading conditions, which complicates analysis of energy dissipation characteristics. Further work on this technique can involve decoupling the creep response from the impact response, introducing temperature control to enable studies at body temperature, and including the visualization of the tissue sample surface via a microscope compatible with the liquid cell.

Rheometry measures the frequency dependent mechanical properties of viscoelastic solids on the macroscale level. The shear moduli components, storage *G*' and loss *G*", can be measured in frequency ranges typically spanning 0.001-0.1 rad/sec to 10-100 rad/sec, depending on the instrument, probe geometry, and sample [13]. For accurate measurement, an amplitude sweep should be performed prior to a frequency sweep to determine the linear elastic range of the material; this is the range of the strain for which *G*' and *G*" remain constant [14,27]. The shear strain chosen for the frequency sweep should be as high as possible within the linear viscoelastic limit (typically 1-2% shear strain) such that sufficient torque is achieved during measurement. The torque during measurements should always be in the allowable range provided by the manufacturer to ensure a sufficient signal to noise ratio.

Additionally, the rheometry probe used should be as large as possible to maximize the torque, but must overlay with the sample completely [13]. In preparing the sample, the tissue should be sliced as flat as possible to minimize stress gradients when contact is made between the plates. When contact is made with the sample, the tissue should not have any water droplets on it to minimize slip at that interface. However, the tissue also must not be dried out prior to or during measurement as this will degrade the tissue structure [13]. The tissue should be fully hydrated with media after contact between both plates. Adhesive, waterproof sandpaper may also be attached to the plates to minimize slip [28]. Additionally, axial compression has been shown to alter the magnitude of *G*' of brain tissue [29]. Since rheology samples are typically thin (~5 mm), small

changes in height (~ 500 µm) may produce large compressive strains (*e.g.*, ~10%), and therefore significant changes in the shear modulus. Moreover, as the sample is viscoelastic, the material will undergo stress relaxation due to axial compression [28], which may affect measurements. Thus, repeated measurements should be performed at similar operating axial strains, and the sample should be allowed to relax (*e.g.,* 5-10 min) prior to measurement. Error associated with these phenomena is a limitation of the technique. Other limitations of rheometry include the assumption that the material is homogeneous and isotropic, which is often not true in tissue samples [13]. Additionally, temperature should be maintained at physiological conditions as it will affect *G*' and *G*" [22]. In brain tissue specifically, increased temperature has been shown to decrease both *G'* and *G"* modestly without changing the power law behavior with frequency, thus following the time-temperature superposition principal [22,30]. Our data are in good agreement with previous studies [22,27] in porcine brain, which observed similar magnitudes of *G*' and *G*", as well as a weak power law frequency dependence in both *G*' and *G*".

The calculated ratio tanδ = *G"/G'* (**Fig. 6**) provides one basis of comparison between rheometry and impact indentation. In impact indentation, we found that brain tissue's energy dissipation capacity increased with increased loading rates. Using rheometry, we found that as frequency increased, tanδ also increased. In other words, the material was more dissipative at higher frequencies. Additionally, while impact indentation measurements do not quantify an elastic modulus directly, the penetration depths x_{max} decrease directly with increasing elastic modulus.

Together, the methods described in this paper enable the mechanical characterization of brain tissue at the micro-, meso-, and macro- length scales, and at different loading rates. The methods presented herein can be used on a number of compliant materials, including both biological tissues and engineered hydrogels. With an in-depth understanding of the multiscale viscoelastic properties of brain tissue, we can better design materials engineered to mimic the mechanical response of the brain. These tissue simulant materials can facilitate prediction of mechanical damage and engineering of protective strategies. Additionally, the material properties of brain can be used to design bioinspired materials for *in vitro* and *in vivo* studies to better understand growth and connectivity of cells in the central nervous system, particularly in the context of neurological diseases such as autism and multiple sclerosis.

Disclosures

The authors have nothing to disclose.

Acknowledgements

We acknowledge support of this work by the National Multiple Sclerosis Society and Simons Center for the Social Brain. BQ acknowledges support from the U.S. National Defense Science & Engineering Graduate Fellowship program.

References

1. van Dommelen, J. A. W., Hrapko, M., & Peters, G. W. M. Mechanical Properties of Brain Tissue: Characterisation and Constitutive Modelling. *Mechanosensitivity of the Nervous System.* 249-281 (2009).
2. Liu, F., & Tschumperlin, D. J. Micro-mechanical characterization of lung tissue using atomic force microscopy. *Journal of Visualized Experiments.* (54), e2911 (2011).
3. Peaucelle, A. AFM-based mapping of the elastic properties of cell walls: at tissue, cellular, and subcellular resolutions. *Journal of Visualized Experiments.* (89), e51317 (2014).
4. Thomas, G., Burnham, N. A., Camesano, T. A., & Wen, Q. Measuring the mechanical properties of living cells using atomic force microscopy. *Journal of Visualized Experiments.* (76), e50497 (2013).
5. Moreno-Flores, S., Benitez, R., Vivanco, M. dM & Toca-Herrera, J. L. Stress relaxation and creep on living cells with the atomic force microscope: a means to calculate elastic moduli and viscosities of cell components. *Nanotechnology.* **21**, 445101 (2010).
6. Desprat, N., Richert, A., Simeon, J., & Asnacios, A. Creep function of a single living cell. *Biophysical Journal.* **88** (3), 2224-33 (2005).
7. Lu, H., Wang, B., Ma, J., Huang, G., & Viswanathan, H. Measurement of creep compliance of solid polymers by nanoindentation. *Mechanics Time-Dependent Materials.* **7** (3/4), 189-207 (2003).
8. Cheng, L., Xia, X., Scriven, L. E., & Gerberich, W. W. Spherical-tip indentation of viscoelastic material. *Mechanics of Materials.* **37**, 213-226 (2005).
9. Kalcioglu, Z., Qu, M., & Van Vliet Multiscale characterization of relaxation times of tissue surrogate gels and soft tissues. *7th Army Science Conference Proceedings.* (2010).
10. Moreno-Flores, S., Benitez, R., Vivanco, M. D., & Toca-Herrera, J. L. Stress relaxation microscopy: Imaging local stress in cells. *Journal of Biomechanics.* **43** (2), 349-354 (2010).
11. Kalcioglu, Z. I., Qu, M., *et al.* Dynamic impact indentation of hydrated biological tissues and tissue surrogate gels. *Philosophical Magazine.* **91** (7-9), 1339-1355 (2011).
12. Kalcioglu, Z. I., Mrozek, R. a, Mahmoodian, R., VanLandingham, M. R., Lenhart, J. L., & Van Vliet, K. J. Tunable mechanical behavior of synthetic organogels as biofidelic tissue simulants. *Journal of Biomechanics.* **46** (9), 1583-91 (2013).
13. Janmey, P. A., Georges, P. C., & Hvidt, S. Basic rheology for biologists. *Methods in Cell Biology.* **83**, 3-27 (2007).
14. Miller, K., & Kurtcuoglu, V. *Biomechanics of the Brain.* Springer Science & Business Media: (2011).
15. Lévy, R., & Maaloum, M. Measuring the spring constant of atomic force microscope cantilevers: thermal fluctuations and other methods. *Nanotechnology.* **13** (1), 33-37 (2002).
16. Fuierer, R. *Basic Operation Procedures for the Asylum Research MFP-3D Atomic Force Microscope. MFP-3D Procedureal Operation "Manualette".* Asylum Research: (2006).
17. Elkin, B. S., Ilankovan, A., & Morrison, B. Age-dependent regional mechanical properties of the rat hippocampus and cortex. *Journal of Biomechanical Engineering.* **132**, 011010 (2010).
18. Elkin, B. S., Azeloglu, E. U., Costa, K. D., & Morrison, B. Mechanical heterogeneity of the rat hippocampus measured by atomic force microscope indentation. *Journal of Neurotrauma.* **24** (5), 812-822 (2007).

19. Lee, E. H., & Radok, J. R. M. The Contact Problem for Visooelastic Bodies. *Journal of Applied Mechanics.* **27** (3), 438-444 (1960).
20. Lin, D. C., Dimitriadis, E. K., & Horkay, F. Robust strategies for automated AFM force curve analysis--I. Non-adhesive indentation of soft, inhomogeneous materials. *Journal of Biomechanical Engineering.* **129** (3), 430-40 (2007).
21. Constantinides, G., Kalcioglu, Z. I., McFarland, M., Smith, J. F., & Van Vliet, K. J. Probing mechanical properties of fully hydrated gels and biological tissues. *Journal of Biomechanics.* **41** (15), 3285-9 (2008).
22. Shen, F., Tay, T. E., *et al.* Modified Bilston Nonlinear Viscoelastic Model for Finite Element Head Injury Studies. *Journal of Biomechanical Engineering -- Transactions of the ASME.* **128** (5), 797-801 (2006).
23. van Dommelen, J. a W., van der Sande, T. P. J., Hrapko, M., & Peters, G. W. M. Mechanical properties of brain tissue by indentation: Interregional variation. *Journal of the Mechanical Behavior of Biomedical Materials.* **3** (2), 158-166 (2010).
24. Rother, J., Nöding, H., Mey, I., & Janshoff, A. Atomic force microscopy-based microrheology reveals significant differences in the viscoelastic response between malign and benign cell lines. *Open biology.* **4** (5), 140046 (2014).
25. Du, P., Lu, H., & Zhang, X. Measuring the Young's Relaxation Modulus of PDMS Using Stress Relaxation Nanoindentation. *Symposium DD - Microelectromechanical Systems - Materials and Devices III.* **1222** (c) (2009).
26. Elkin, B. S., & Morrison, B. Viscoelastic properties of the P17 and adult rat brain from indentation in the coronal plane. *Journal of Biomechanical Engineering.* **135**, 114507 (2013).
27. Brands, D. W., Bovendeerd, P. H., Peters, G. W., Wismans, J. S., Paas, M. H., & van Bree, J. L. Comparison of the dynamic behavior of brain tissue and two model materials. *43rd Stapp Car Crash Conference Proceedings.* 313-320 (1999).
28. Hrapko, M., van Dommelen, J. A. W., Peters, G. W. M., & Wismans, J. S. H. M. Characterisation of the mechanical behaviour of brain tissue in compression and shear. *Biorheology.* **45** (6), 663-76 (2008).
29. Pogoda, K., Chin, L., *et al.* Compression stiffening of brain and its effect on mechanosensing by glioma cells. *New Journal of Physics.* **16** (7), 075002 (2014).
30. Peters, G. W. M., Meulman, J. H., & Sauren, A. A. H. J. The applicability of the time/temperature superposition principle to brain tissue. *Biorheology.* **34** (2), 127-138 (1997).

